Mapping and ablation of atrial tachyarrhythmias : from signal to substrate

Groot, N.M.S. de

chapter

10

3-D Distribution of Bipolar Atrial Electrogram Voltages in Patients with Congenital Heart Disease

Natasja M. S. de Groot, Aaf F. M. Kuijper, Nico A. Blom,
Marianne Bootsma, Martin J. Schalij

Abstract

Introduction: Voltage differences might be used to distinguish normal atrial tissue from abnormal atrial tissue. This study was aimed at identifying lowest voltage areas in patients with atrial tachycardia after surgical correction of congenital heart disease and to evaluate whether identification of these areas in diseased hearts facilitates selection of critical conduction pathways in reentrant circuits as target sites for catheter ablation.

Methods and Results: Ten patients (4 male, 39 ± 15 yr) with normal sized atria and atrio-ventricular reciprocating tachycardia (control group) and ten patients (5 male, 32 ± 7 yr.) with congenital heart disease and post-operative atrial tachycardia (CL = 281 ± 79 ms) referred for radiofrequency catheter ablation were studied. Mapping and ablation was guided by a 3-D electro-anatomical mapping system (CARTO) in all patients. In the control group, voltage maps were constructed during sinus rhythm and during tachycardia to evaluate the voltage distribution. The amplitude of bipolar signals was 1.90 ± 1.45 mV (0.11-8.12 mV, n = 660) during sinus rhythm and 1.45 ± 1.66 mV (0.12-5.83 mV, n = 440, $p < 0.05$) during atrio-ventricular reciprocating tachycardia. In the study group, the amplitude of 1962 bipolar signals during tachycardia was 1.01 ± 1.19 mV (0.04-9.40 mV), which differed significantly from the control group during tachycardia ($p < 0.0001$). No significant difference in the tachycardia cycle length between the control and study group was found ($p < 0.05$).
As the lowest voltage measured in normal hearts was 0.1 mV, this value was used as the upper limit of the lowest voltage areas in the patients with congenital heart disease. These areas were identified by detailed voltage mapping and represented by a gray color. Activation and propagation maps were then used to select critical conduction pathways as target sites for ablation. These sites were characterized by fragmented signals in all patients. Ablation resulted in termination of the tachycardia in 8/10 (80%) patients. Complications were not observed.

Conclusion: Identification of the lowest voltage areas using a cut-off value of 0.1 mV in congenital heart disease patients with post-operative atrial reentrant tachycardia facilitated the selection of critical conduction pathways as target sites for ablation.

Introduction

Atrial tachy-arrhythmias after surgery for congenital heart disease have become a more frequently encountered clinical problem since patients with congenital heart disease have an improved life expectancy due to the good results of surgical interventions.[1-4] Reentry is the mechanism causing most of these arrhythmias.[5,6] In these patients, delineation of the reentrant circuit is often difficult, as these circuits may be complex with multiple exits, entrances, dead-end pathways and bystander-loops. This is the result of enlarged atria with distortion of the anatomy by, for example, incisions, patches, baffles, and conduits.[7,8]

Drug therapy, still the first choice treatment modality in most patients, is associated with high recurrence rates. [5] If the arrhythmia recurs, anti-tachycardia pacing or radio-frequency catheter ablation (RFCA) may serve as alternative treatment modalities.[9-11] RFCA of post-operative atrial tachycardia is targeted at areas of slow conduction, which can be identified, by fragmented intra-cardiac signals and entrainment with concealed fusion.[12-14] The target areas for ablation are typically bounded by anatomical barriers such as the AV annulus and surgical suture lines. [15]

Accurate localization of these structures is therefore mandatory for successful ablation. To facilitate 3-D reconstruction of the atria in these patients, the CARTO electro-anatomical mapping system can be used.[16-21]

Areas of abnormal atrial tissue can also form the border of a critical conduction pathway in a reentrant circuit.[21] To distinguish normal atrial tissue from abnormal atrial tissue voltage differences might be used. As the CARTO system allows on-line construction of color-coded 3-D voltage maps, these maps can be used to identify low voltage areas, that are scattered throughout the atrial wall and difficult to localize by a fluoroscopically guided mapping technique.[21]

However, until now, no study has compared the voltage distribution between patients with normal and abnormal hearts. Therefore we evaluated the distribution of bipolar signal voltages in patients with normal hearts and atrio-ventricular reciprocating tachycardia and in patients with atrial tachycardia after surgical correction of congenital heart disease in order to determine a cut-off value for the lowest voltage areas in abnormal hearts. Our objective was to determine whether identification of these lowest voltage areas facilitates the selection of critical conduction pathways in the reentrant circuits of patients with post-operative tachycardia prior to ablation.

Methods

Study Group

The study population consisted of 10 patients with atrial tachycardia after surgical repair of congenital heart disease referred for RFCA. Prior to ablation, all patients underwent full cardiac examination including 24-hour Holter monitoring and echocardiography. An electrophysiological study was performed prior to the ablation procedure. Data regarding cardiac diagnosis, surgical procedures, previous arrhythmias, usage of anti-arrhythmic drugs, were obtained from patient files. During the procedure, Heparin was administered intravenously to maintain an anti-clotting time of 2.5-3 times the control value for adequate anticoagulation. Systemic blood pressure and heart rate were monitored continuously. If necessary, patients were sedated with Midazolam and Fentanyl intravenously.

Control Group

The control group consisted of 10 patients referred for RFCA of an accessory pathway. None of these patients had undergone prior cardiac surgery.
In both the control and study group, anti-arrhythmic drugs were discontinued at least 3 days prior to ablation.

Mapping System

Endocardial mapping was performed with the CARTO 3-D electro-anatomical mapping system (Biosense Webster, USA).[17,18] A 7F Navi-Star catheter (Biosense Webster,USA) with a 7F 4 mm tip was used as mapping and ablation catheter. The tip of the catheter contains 2 bipolar electrode pairs with an inter-electrode distance of 2 mm. Recordings from a quadripolar 6F diagnostic catheter (Biosense Webster, USA) positioned into either the right atrial appendage or the coronary sinus were used as a electric timing reference. After amplification and filtering (bandwidth 10-400 Hz) the signals were multiplexed and displayed on a computer monitor. Programmed electrical stimulation applying up to three extra-stimuli was performed with a constant current stimulator (Medtronic, USA) using pacing stimuli at twice diastolic threshold with a 2 ms pulse width.

Mapping Procedure

After localization of anatomical landmarks (e.g. superior caval vein, tricuspid valve, His bundle and surgical conduits), 3-D electro-anatomical activation and voltage maps of the right atrium were constructed by sequential recording of signals at multiple sites. A data point was accepted only when the variability in cycle length, local activation time and maximum beat to beat difference of the catheter's location were less than 2 % and 3 ms and 4 mm respectively. These parameters, combined with fluoroscopy and impedance measurements were used to exclude signals with low amplitudes due to poor contact of the catheter's tip with the endocardial wall. Moving the catheter's tip until the icon on

the screen bended against the virtual atrial wall further ensured the contact with the endocardial wall.

Activation maps were constructed by determining the local activation time for each recorded bipolar signal relative to the electric timing reference. Maximum amplitude of the bipolar signal was used to define the local activation time. The amplitude of the bipolar signals were measured automatically and used to construct voltage maps.

Points indicating anatomical structures were defined as location only and their amplitude was not taken into account. Activation and voltage maps of the right atrium were obtained in the control group during both sinus rhythm and tachycardia. Frequency distribution histograms were used to compare the frequency distributions of the signal's amplitude during sinus rhythm and atrio-ventricular reciprocating tachycardia. This frequency distribution was assumed to represent the range of amplitudes of bipolar signals present in normal atria.

In the study group, voltage maps were only constructed during tachycardia. The right atrium was mapped in all patients. In patients who underwent a Mustard procedure, the left atrium was mapped also.

The lower limit of voltages found in the control group was used as the upper limit for the lowest voltage signals in the study group. Low voltage electrogram areas (<cut-off value) were gray-colored and labeled as scar tissue, thereby signifying the most diseased areas of atrial tissue. Finally, by combining information obtained from voltage –, activation –, and propagation-maps, critical conduction pathways which are central common pathways of the reentry circuit, were identified. These sites were target sites for RFCA.

Radiofrequency Ablation Procedure

After voltage- and activation- mapping, a temperature controlled radiofrequency catheter ablation was performed (maximum tip temperature set at 70° C). Ablation was aimed at creating lines of conduction block between anatomically or surgically created conduction barriers or between zones identified as scar tissue. Ablation was continued until the tachycardia was terminated and no longer inducible.

Statistical analysis

All data are expressed as mean values ± SD. An independent two-sample T test was used to compare the tachycardia cycle length between the control group and study group.

An unequal independent T-test was used to compare 1) the amplitude of bipolar signals recorded during sinus rhythm and tachycardia in the control group and 2) the mean amplitude of bipolar signals between the control group and study group during tachycardia. Statistical significance was defined as $p < 0.05$.

Table 1. **Patient characteristics**	
Number	10
Male/ female	5/5
Age	32 ± 7 yr.
left atrial dimension (echocardiography)	5.0 ± 0.9 cm
interval operation-arrhythmia	17 ± 5 yr.

Table 2. **Patient pathology operation age at the time number of of the operation operations**				
1	transposition great arteries	Mustard	3	2
2	tricuspid atresia (type IB)	Fontan	7	2
3	tricuspid atresia (type IIB)	Fontan	1	2
4	tricuspid atresia	Fontan	3	4
5	atrial septal defect	closure defect	5	2
6	double inlet ventricle	Fontan	14	2
7	transposition great arteries	Mustard	1	2
8	atrio-ventricular septal defect	closure defect	15	2
9	transposition great arteries	Mustard	1	1
10	tricuspid atresia	Fontan	9	1

Table 3. **Patient antiarrhythmic drug failed pacemaker lead AR drugs system**				
1	verapamil	1	AAI	endocardial
2	amiodarone	3	AAI	endocardial
3	amiodarone	4	AAI	epicardial
4	amiodarone	1	–	–
5	digoxin	1	–	–
6	–	3	–	–
7	–	2	–	–
8	sotalol	3	–	–
9	sotalol	2	–	–
10	sotalol	1	–	–

Table 4.					
Patient	**CL (ms)**	**Points N**	**Total Activation Time (ms)**	**Procedure time (min)**	**Fluoroscopy Time (min)**
1	417	236	385	320	70
2	245	203	285	300	64
3	434	216	411	296	44
4	225	173	131	100	7
5	270	192	308	315	17
6	266	330	316	253	51
7	236	192	214	230	35
8	270	184	267	228	23
9	250	242	250	360	67
10	200	202	200	276	42
± SD	281 ± 75	217 ± 43	277 ± 80	268 ± 68	42 ± 21

Results

Study population

The characteristics of the study group (n = 10, 32 ± 7 yr, 5 male) are summarized in Table I. The anatomy before surgery included: Atrio-ventricular septal defect (1); Atrial septal defect (1); Transposition of the great arteries (3); Double inlet ventricle (1); and Tricuspid atresia (4). The age at the time of the initial operation ranged from 1-15 (6 ± 5) years. The surgical procedures (Table II) included: closure of an atrial septal defect with a Dacron patch (1); closure of an atrio-ventricular septal defect (1); Mustard (3) and Fontan (5) procedures. Additional procedures preceding the Fontan operation included a classical Glenn operation and the construction of a Blalock shunt.[22,23] Conduit replacement was performed in two patients.

The interval from the time of the initial operation to the onset of the arrhythmia ranged from 10 to 26 (17 ± 5) years. Before the ablation procedure, 8 patients used anti-arrhythmic drugs and a pacemaker was implanted in 3 patents (Table III).

Control Group

All ten patients (39 ± 15 yr, 4 male) had normal sized atria as established by echocardiography and had no history of atrial flutter or atrial fibrillation.

Mapping Procedure

In the control group, right atrial activation maps were constructed during sinus rhythm (CL = 749 ± 153 ms) and tachycardia (CL = 325 ± 54 ms). The sinus rhythm and tachycardia activation maps consisted of respectively 75 ± 37 and 53 ± 24 points with a total activation time of 143 ± 68 ms and 91 ± 46 ms. The amplitude of 660 bipolar signals recorded during sinus rhythm was 1.90 ± 1.45 (0.11-8.12) mV whereas the amplitude of 440 bipolar signals recorded during tachycardia was 1.45 ± 1.66 (0.12-5.83) mV (Figures 1 and 2). The amplitude of the remaining points was not taken into account as they represented anatomical structures. There was a significant difference between the amplitude of bipolar signals during sinus rhythm and tachycardia ($p < 0.05$). Activation maps were obtained in all patients with congenital heart disease during tachycardia (CL = 281 ± 75 ms, Table IV). These activation maps consisted of 217 ± 43 points with a total activation time of 277 ± 80 ms. The amplitude of 1962 bipolar signals recorded during tachycardia was 1.01 ± 1.19 (0.04-9.40) mV and differed significantly from the control group during tachycardia ($p < 0.0001$). No significant difference in the tachycardia cycle length between the control and study group was found ($p < 0.05$). Again, the amplitude of points indicating anatomical structures was not taken into account. As can be seen in Figure 3 the frequency distribution of the bipolar electrogram voltages shifted to lower values in the study group as compared to the control group.

In the control group, the amplitude of the recorded bipolar signals, both during sinus rhythm and tachycardia, was never lower than 0.1 mV. This value was therefore used as a

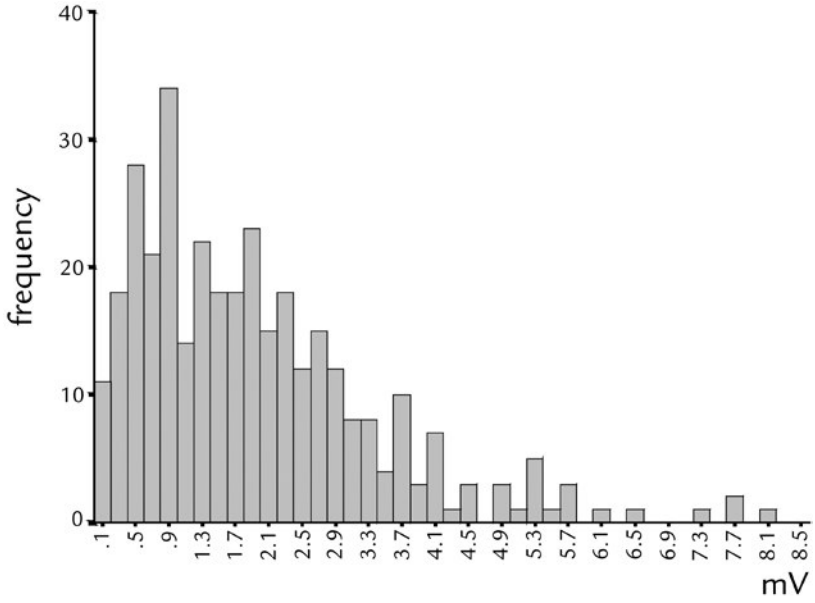

Figure 1.

Frequency distribution of the amplitude of bipolar signals during sinus rhythm in the control group. The amplitude of 660 bipolar signals recorded during sinus rhythm was 1.90 ± 1.45 (0.11-8.12) mV. No signals with an amplitude of < 0.1 mV were recorded.

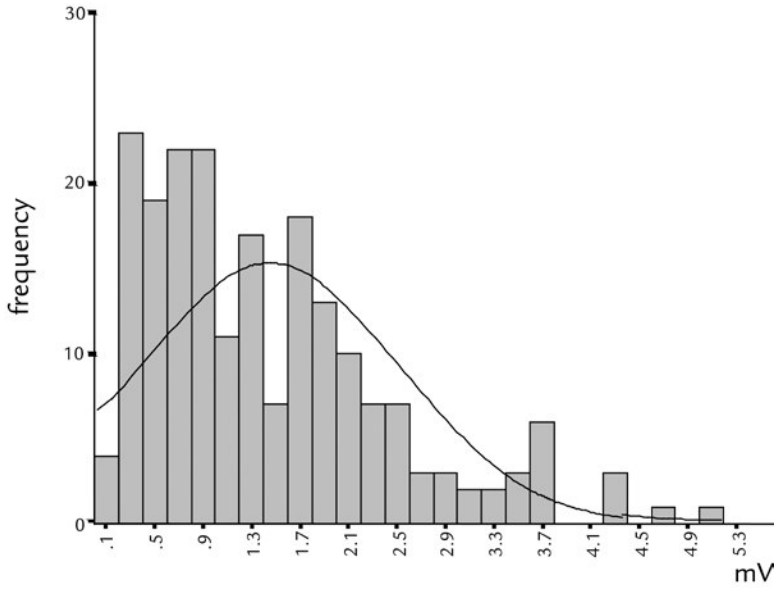

Figure 2.

Frequency distribution of the amplitude of bipolar signals during tachycardia in the control group. The amplitude of 440 bipolar signals recorded during tachycardia was 1.45 ± 1.66 (0.12-5.83) mV. Again, no signals with an amplitude of <0.1 mV were recorded.

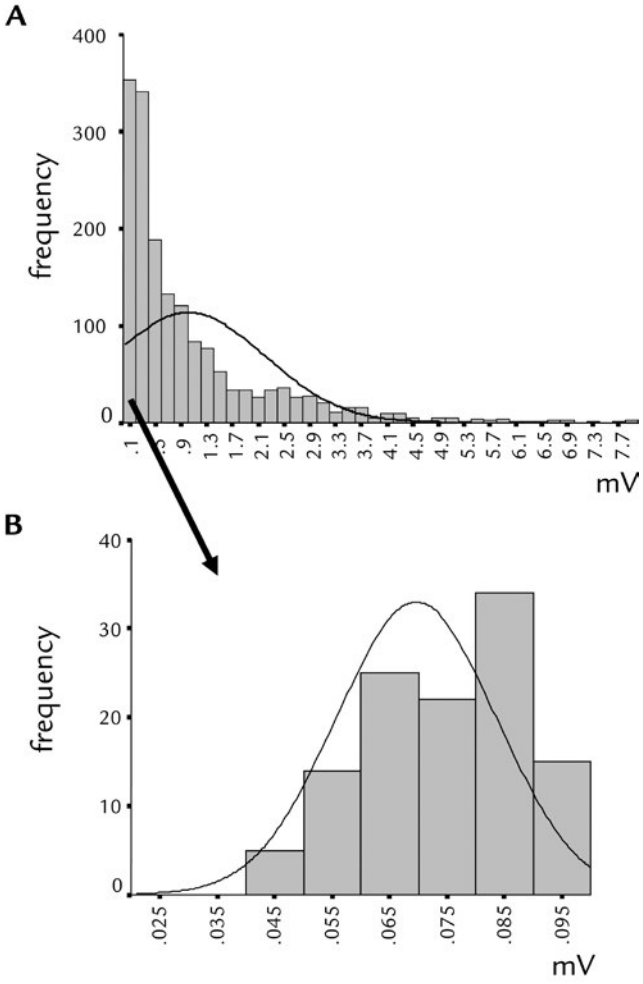

Figure 3.

Frequency distribution of the amplitude of bipolar signals during tachycardia in the study group. The amplitude of 1962 bipolar signals recorded during tachycardia was 1.01 ± 1.19 (0.04-9.40) mV. ± 10% of signals recorded had an amplitude of < 0.1 mV.

cut-off value for the lowest voltage areas in the study group. These low voltage areas (< 0.1 mV) were marked as scar tissue, and comprised 11 ± 4 % of the points sampled from the endocardial surface of the atria in patients with congenital heart disease.

An example of a right atrial voltage map recorded during tachycardia (CL = 435 ms) in a patient after a Fontan procedure is shown in Figure 4 (panel A, antero-posterior view). The tricuspid valve and inferior caval vein were marked. Corresponding high and low voltage signals are shown. The amplitudes of these signals ranged from 0.01 mV to 3.69 mV. Bipolar atrial signals with amplitudes <0.1 mV were labeled as scar tissue (gray colored

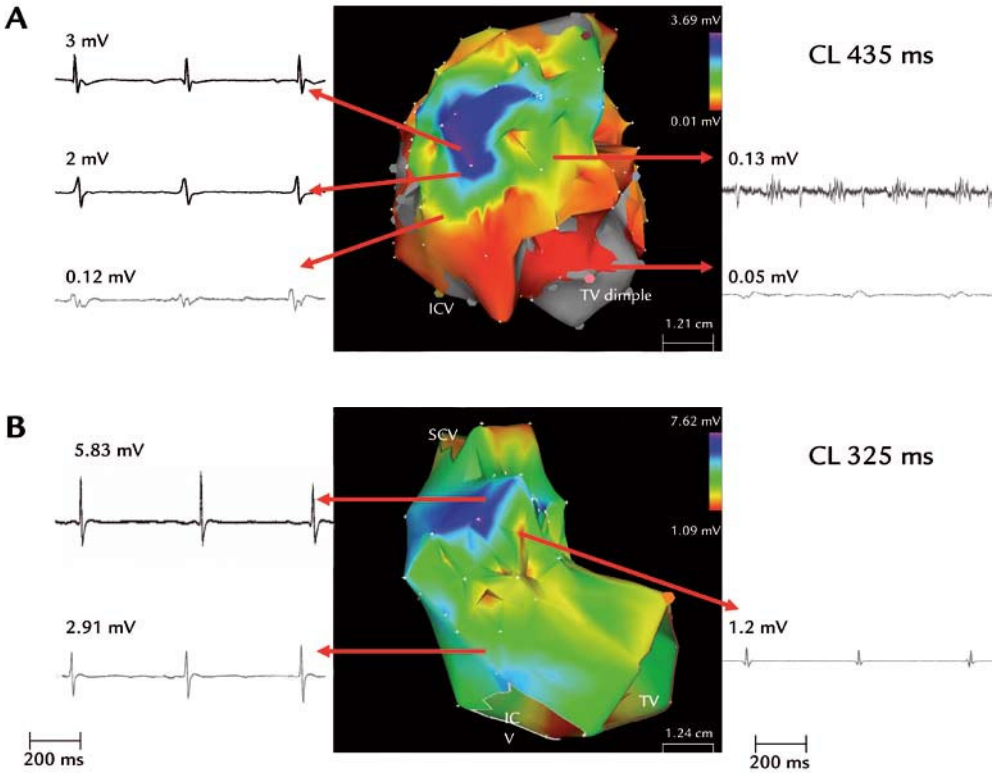

Figure 4.

Scar tissue mapping. The amplitudes of the recorded bipolar signals are indicated by the color legend at the top of the map. *Panel A:* A right atrial voltage map in the antero-posterior view recorded in a patient with a tricuspid atresia who underwent a Fontan procedure is shown. Low voltage areas are colored orange where as high voltage areas are colored purple. Bipolar atrial signals with amplitudes <0.1 mV were defined as scar tissue and represented by the gray colored areas. Corresponding high and low voltage signals are shown.
Panel B: A right atrial voltage map recorded during tachycardia in a patient who underwent RFCA of an accessory pathway is shown in the antero-posterior view (*panel B*). No areas with amplitudes of < 0.1 mV were recorded. Corresponding signals recorded in this patient are shown.
SCV = superior caval vein, ICV = inferior caval vein, TV = tricuspid valve markings.

areas). A right atrial voltage map recorded during tachycardia (CL = 325 ms) in a patient with a normal heart who underwent RFCA of an accessory pathway is shown in panel B (antero-posterior view). No low voltage areas (<0.1 mV) were recorded. Corresponding signals recorded are shown; the lowest amplitude recorded in this patient was 1.09 mV.
Figure 5 gives the computer reconstructed propagation map during tachycardia (same patient shown in figure 4). The yellow line indicates the direction of the activation wave front. A counterclockwise propagating wave front conducted slowly through the narrow isthmus between the areas of scar tissue, before activating the remaining part of the RA. During RF ablation, a line of block was created between the 2 areas of scar tissue. During ablation, tachycardia was terminated and non-inducible.

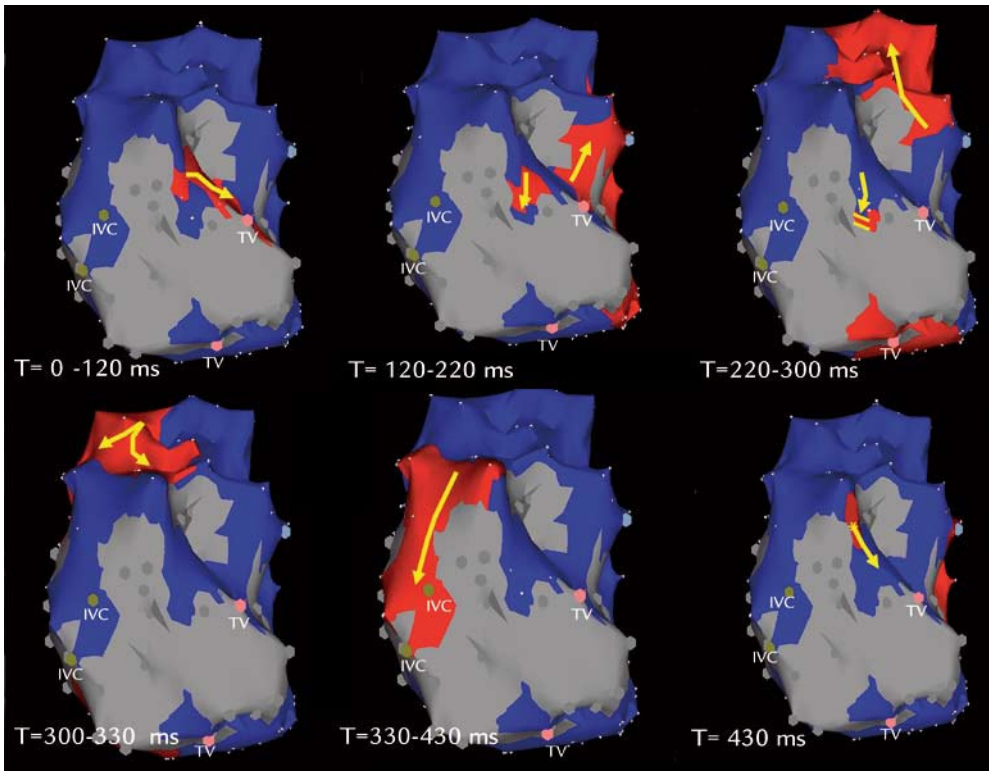

Figure 5.
Propagation maps during tachycardia recorded in the same patient shown in figure 4. The red areas represent activated regions and the blue areas represent non-activated regions. The yellow arrows indicate the direction of the wave front. A counter clockwise propagating wave front conducted slowly through a pathway (yellow star) between 2 areas of scar tissue. RF ablation of this slowly conducting isthmus resulted in termination of the tachycardia.
SCV = superior caval vein, ICV = inferior caval vein, TV = tricuspid valve marking.

After the careful reconstruction of voltage and propagation maps, RF current was applied at areas of slow conduction bounded by scar tissue, anatomical structures, or surgical suture lines. Each ablation site was marked, which facilitated the creation of complete lines of conduction block. In this way, by selecting target sites for RFCA using both voltage-, activation- and propagation maps, application of RF energy resulted in termination of the tachycardia in 8/10 patients (80 %). In the 2 remaining patients, RF ablation resulted in the induction of another and faster tachycardia. DC-shock cardioversion was necessary in these 2 patients to restore sinus rhythm. In both patients, extensive areas of scar tissue were found throughout the RA.

In the patient with an atrial septal defect the line of block was created between two areas of scar tissue in the inferior part of the RA. In the patient with the atrio-ventricular septal defect the line of block was created between the tricuspid valve and the inferior caval vein. In 5 patients who had undergone a Fontan procedure a line of block was created either between 2 areas of scar tissue or between a scar tissue area and the atrio-pulmonary conduit. Successful target sites for RFCA in three patients who had undergone a Mustard procedure were located along the baffle and between areas of scar tissue located in the anterior wall of the RA.

The mean procedure and fluoroscopy time was respectively 255 ± 73 min and 39 ± 23 min. No procedural complications were observed.

Follow-up

After a follow-up period of 12 ± 3 (3-11) months, one patient (with a tricuspid atresia after a Fontan procedure) and had undergone a unsuccessful ablation procedure, died due to hemodynamic deterioration during an episode of pneumonia (5 months after the ablation procedure). No recurrences were observed in the other patients.

Discussion

We reported the use of a 3-D electro-anatomical mapping system (CARTO) for evaluation of differences in the distribution of bipolar signal voltages in patients with normal hearts during sinus rhythm and during atrio-ventricular reciprocating tachycardia and in patients with atrial tachycardia after surgical repair of congenital heart disease. From these data we defined a cut-off value for the lowest voltage areas, which were subsequently labeled as scar tissue in the congenital heart disease patients. Delineation of these areas of scar tissue facilitated RFCA of post-operative atrial arrhythmias.

RFCA of post-operative reentrant tachycardia may be guided by conventional mapping techniques, 3-D electro-anatomical mapping or non-contact mapping.[6,7,21,24,25] Conventional mapping however is time consuming, and require long fluoroscopy times.[9] Furthermore, multiple catheters are often required in order to locate the reentrant pathway accurately.[15]

Regardless the mapping technique used, the major problem of mapping post-operative atrial tachyarrhythmias, is the exact anatomical location of scar tissue and other structures in the atrium (like conduits). As scar tissue may serve as the border of a critical conduction pathway in a reentrant circuit, it is of importance to delineate it correctly. Because of the fact that the atria of these patients are often diffusely diseased low amplitude fragmented signals can be recorded at multiple sites. To discriminate scar tissue from diseased but conducting tissue, Dorostkar et al. first used the CARTO system in operated congenital heart disease patients with atrial tachyarrhythmias.[20] They introduced the so-called patch index, which is the ratio of the local impedance divided by the amplitude of the local signal, as scar tissue is characterized by a high electrical impedance and a low amplitude of the signal. From this study it became clear that a value of > 200 Ω/mV correlated with either patch or diseased tissue and a value of 100 Ω/mV correlated with normal cardiac tissue. However, it is not possible (with the CARTO system) to automatically calculate this patch index on-line, therefore the patch index is not suitable for identification of scar tissue during an ablation procedure.

As the voltage of the recorded signals is displayed on-line, voltage mapping may serve as an alternative approach to identify the lowest voltage areas. The use of unipolar signals, by reflecting local electrical activity more accurately than bipolar signals, may be prefered. However, the quality of unipolar signals is often negatively affected by electromagnetic interference from equipment in the catheterization laboratory.[26] This interference makes it often difficult to distinguish fractionated low-amplitude signals, representing local electrical activity, from far-field electrical activity. Therefore in this study, we used bipolar signals. The amplitude of bipolar signals is in general influenced by the area of a dipole layer, the distance between the dipole and the recording electrode, properties of the underlying tissue, recording techniques, the inter-electrode distance, and the angle between the activation wave front and the recording electrodes.[27] The different angles between

the activation wave fronts and the recording electrodes during sinus rhythm and during tachycardia may explain the difference in voltage distributions found in the control group during sinus rhythm and during tachycardia. Furthermore the high rate during tachycardia may be responsible for the lower voltage (1.90 ± 1.45 mV during sinus rhythm, 1.45 ± 1.66 mV during tachycardia, $p < 0.05$).

Comparing the results of the study group with the results of the control group, in which the recording techniques and the inter-electrode distances were identical and assuming a statistically similar distribution of angles between the wave fronts and the recording electrodes, the different voltage distribution can only be explained by differences in the properties of the underlying atrial tissue or by differences in the distance between the bipolar recording electrode and the atrial tissue.

As the lowest voltage recorded in the control group during sinus rhythm and during tachycardia, was respectively 0.11 mV and 0.12 mV, we have defined 0.1 mV as the cut-off value of the lowest voltage signals. Each site at which a voltage of <0.1 mV was recorded was therefore marked as scar tissue. Using this cut-off value, 11 ± 4% of the points sampled from the endocardial surface were labeled as scar tissue in patients with congenital heart disease. As shown, scar tissue was found in more or less circumscribed areas throughout the atria and was not limited to surgical suture lines, patches, baffles or conduits only. The importance of demarcating regions of scar tissue prior to ablation is supported by the observation that in all patients scar tissue formed at least one border of a critical conduction pathway during reentry.

Recently, Nakagawa and Jackman also demonstrated that delineation of scar tissue by voltage mapping might facilitate RFCA of atrial tachycardia. However they used a cut-off value of 0.5 mV.[21] As shown in **Figure 3**, the use of this cut-off value in our patients would have resulted in a significant increase of the low-voltage areas. Consequently we would have missed some of the slow conduction pathways (**Figure 4** A and **Figure 5**) critical for the perpetuation of the reentrant tachycardia. Therefore, although the cut-off value of 0.1 mV may have resulted in an underestimation of the area of scar tissue, in combination with the activation and propagation maps it allowed us to reconstruct a reentrant pathway in all patients.

In patients with congenital heart disease, structural damage of atrial myocardium is caused by prior surgical interventions and/or hemodynamical overload. As a consequence of this, separation of myocardial fibers by interposition of fibrous tissue occurs.[28] This deposition of fibrous tissue gives rise to low-amplitude, fractionated signals as it results in widely separated myocardial fiber which are activated asynchronously.[29] As shown, the critical conduction pathways, being target sites for RFCA, exhibited fractionated activity, indicating areas of slow and asynchronous conduction. In conclusion, accurate localization of anatomical structures by voltage mapping and detailed activation mapping are equally important to reveal the exact reentrant pathway in these patients.

Clinical Implications

Previous studies showed that target sites for RFCA in patients with post-operative atrial reentrant arrhythmias are frequently located between anatomical structures and surgically created barriers like atrio-pulmonary conduits, atriotomy scars, patches and baffles.[15] The results of our study emphasize the role of low voltage areas as they may serve as borders of a critical conduction pathway within a reentrant circuit. Therefore, 3-D scar tissue mapping combined with activation and propagation maps may enhance the results of RFCA of atrial tachy-arrhythmias in congenital heart disease patients.

Study Limitations

Although we used a number of different methods, as described above, to exclude poor contact signals, some low amplitude signals could have been the result of poor contact of the catheter's tip with the endocardial wall.

In most studies regarding RFCA of post-operative atrial reentrant arrhythmias, selection of target sites was based on entrainment techniques.[15] We did not use this technique as pacing often did not result in capture of the myocardium and entrainment of these complex reentrant circuits may cause a change in the reentrant pathway or results in the induction of atrial fibrillation. If this occurs, a new activation map should be constructed resulting in a significant prolongation of the procedure time.

Patients in the study group were only studied during tachycardia as most patients had already a tachycardia at the beginning of the ablation procedure. Construction of an activation map during sinus rhythm would have prolonged the procedure time and was therefore not performed.

Though the initial results were promising, larger studies with a longer follow-up period will be necessary to evaluate the long-term outcome of RFCA of post-operative atrial reentrant tachycardias in congenital heart disease patients.

Conclusion

RFCA may be a successful treatment modality in congenital heart disease patients with post-operative atrial reentrant arrhythmias. Three-dimensional scar tissue mapping, as described in this study, using a cut-off value of 0.1 mV for the discrimination between scar tissue and conducting tissue in combination with activation- and propagation-maps facilitated the outcome of RFCA in these patients.

References

1. Hayes CJ, Gersony WM. Arrhythmias after the Mustard operation for transposition of the great arteries: a long-term study. J Am Coll Cardiol 1986; 7: 133-7.
2. Fishberger SB, Wernovsky G, Gentles TL, Gauvreau K, Burnett J, Mayer JE, Walsh. EP factors that influence the development of atrial flutter after the Fontan operation. J Thorac Cardiovasc Surg 1997;113: 80-86.
3. Driscoll DJ, Offord PO, Feldt RH, Schaff HV, Puga FJ, Danielson GK. Five- to fifteen-year follow-up after Fontan operation. Circulation 1992;85:469-96.
4. Vetter Vl, Horowitz LN. Electrophysiologic residua and sequelae of surgery for congenital heart defects. Am J of Cardiol 1982;50:588-601.
5. Haines DE, DiMarco JP. Sustained intraatrial reentrant tachycardia: clinical, electrocardiographic and electrophysiologic characteristics and long-term follow-up. J Am Coll Cardiol1990;15:1345-54.
6. Lesh MD, Van Hare GF, Epstein LM, Fitzpatrick AP, Scheinman MM, Lee RJ, Kwasman MA, Grogin HR, Griffin JC. Radiofrequency catheter ablation of atrial arrhythmias. Results and mechanisms. Circulation 1994; 89: 1074-89.
7. Triedman JK, Saul JP, Weindling SN, Walsh EP. Radiofrequency ablation of intra-atrial reentrant tachycardia after surgical palliation of congenital heart disease. Circulation 1995;91:707-714.
8. Cronin CS, Glick DB, Nitta T, Mitsuno M, Boineau JP, Cox JL. Surgical ablation of atrial flutter after the Mustard procedure. Pace 1994;17:745.
9. Van Hare GF, Lesh MD, Stanger P. Radiofrequency catheter ablation of supraventricular arrhythmias in patients with congenital heart disease: results and technical considerations. JACC 1993;22: 883-90.
10. Van Hare GF, Lesh MD, Bertrand AR, Perry JC, Dorostkar PC. Mapping and radiofrequency ablation of intraatrial reentrant tachycardia after the Senning or Mustard procedure for transposition of the great arteries. Am J Cardiol 1996:77:985-991.
11. Balaji S, Johnson TB, Sade RB, Case CL, Gilette PC. Management of atrial flutter after the Fontan procedure. J Am Coll Cardiol 1994; 23:1209-1215.
12. Cruz FS, Fagundes M, Boghossian S, Ribeiro JC, Van Heusden L, Maia IG. A comparison of radiofrequency ablation of common type and atriotomy scar related atrial flutter. Pace 1995;20:860.
13. Lesh MD, Van Hare GF. Status of ablation in patients with atrial tachycardia and flutter. Pace 1994;17:1026-33.
14. Van Hare GF, Lesh MD. Atrial tachyarrhythmias after the Senning or Mustard procedure: preliminary experience with concealed entrainment mapping and radiofrequency (RF) ablation. Pace 1994;17:745.
15. Kalman JM, VanHare G, Olgin JE, Saxon LA, Stark SI, Lesh MD. Ablation of 'incisional' reentrant atrial tachycardia complicating surgery for congenital heart disease: Use of entrainment to define a critical isthmus of conduction. Circulation 1996; 93: 502-512.
16. Shpun S, Gepstein L, Hayam G, Ben-Haim SA. Guidance of radiofrequency endocardial ablation with real-time three-dimensional magnetic navigation system. Circulation 1997;96:2016-2021.
17. Smeets JLRM, Ben-Haim SA, Rodriguez LM, Timmermans C, Wellens HJJ. New Method for Nonfluoroscopic Endocardial Mapping in Humans: Accuracy Assessment and First Clinical Results. Circulation 1998 97: 2426-2432.
18. Gepstein L, Hayam G, Ben-Haim SA. A novel method for nonfluoroscopic catheter- based electroanatomical mapping of the heart - In vitro and in vivo accuracy results. Circulation 1997;95:1611-1622.
19. Delacretaz E, Stevenson WG, Ganz LI, Landzberg MJ, Ellison KE, Friedman PL. Entrainment mapping combined with 3D electroanatomic mapping for ablation of multiple atrial macroreentry circuits in adults with repaired congenital heart disease. Pace 1999;22:892.
20. Dorostkar PC, Cheng JIE, Scheinman MM. Electroanatomical mapping and ablation of the substrate supporting intraatrial reentrant tachycardia after palliation for complex congenital heart disease. Pace 1998;21:1810-1819.
21. Nakagawa H, Jackman WM. Use of a 3-dimensional electroanatomical mapping system for catheter ablation of macroreentrant right atrial tachycardia following atriotomy. J of Electrocardiology 1999;32:S16-21.

22. Arciniegas E, Farooki ZQ, Hakimi M, Perry BL, Green EW. Classic shunting operations for congenital cyanotic heart defects. J Thorac Cardiovasc Surg 1982;84:88-96.
23. Di Carlo D, Williams WG, Freedom RM, Trusler GA, Rowe RD. The role of cava-pulmonary (Glenn) anastomosis in the palliative treatment of congenital heart disease. J Thorac Cardiovasc Surg 1982; 83(3):437-42.
24. Lin AC, Kall JG, Kopp DE, Johnson T, Burke MC, Arruda M, Verdino RJ, Wilber DJ. Mechanism of arrhythmias after surgical repair of atrial septal defect. Pace 1999; 22:704.
25. Betts T, Allen S, Salmon A, Edwards T, Morgan J. Characterization of atrial tachycardia in patients after Fontan surgery using a non-contact mapping system. Pace 1999;22:721.
26. Blanchard SM, Damiano RJ, Asano T. The effects of distant electrical events on glocal activation in unipolar epicardial electrograms. IEEE Trans Biomed Engineer 1987;34:539.
27. Biermann M, Sheanasa M., Borggrefe M, Hindricks G, Haverkamp W, Breithardt G. The interpretation of cardiac electrograms. In Cardiac Mapping. New York, Futura Publishing:1993 ;11-34.
28. Spach MS, Miller WT, Dolber PC. The functional role of structural complexities in the propagation of depolarization in the atrium of the dog: cardiac conduction disturbances due to discontinuities of effective axial resistivity. Circ Res 1982; 50:175.
29. Roberts DE, Scher AM. Effect of tissue anisotropy on extracellular potential fields in canine myocardium in situ. Circ Res 1982; 50: 342-351.